Received: 16 April 2018 | Revised: 4 June 2018 | Accepted: 27 June 2018
DOI: 10.1002/sat.1272

WILEY

RESEARCH ARTICLE

Standardized testing conditions for satellite communications on-the-move (SOTM) terminals

Mostafa Alazab Elkhouly[1,2] | Jonas König[1,2] | Niklas Beuster[1] | Florian Raschke[2] | Alexander Ihlow[1] | Colin Robinson[3] | Raul Orus-Perez[4] | Fritz Schurig[5] | Andreas Knopp[6] | Albert Heuberger[2] | Markus Landmann[2] | Giovanni Del Galdo[1,2]

[1]Electronic Measurements and Signal Processing, Technische Universität Ilmenau, Ilmenau, Germany
[2]Fraunhofer Institute for Integrated Circuits IIS, Erlangen, Germany
[3]Mutual Recognition Arrangement Working Group, Global VSAT Forum (GVF), Washington, District of Columbia
[4]Electromagnetics and Space Environment Division, European Space Agency (ESA/ESTEC), Noordwijk, The Netherlands
[5]Operations Division, EUTELSAT S.A., Paris, France
[6]Chair of Signal Processing, Bundeswehr University Munich, Germany

Correspondence
Mostafa Alazab Elkhouly, Fraunhofer Institute for Integrated Circuits IIS, Am Wolfsmantel 33, D-91058 Erlangen, Germany.
Email: mostafa.elkhouly@iis.fraunhofer.de

Funding information
European Space Agency

Summary

Performance validation of Satcom on-the-move (SOTM) terminals is becoming more important as the satellite operators continue to recognize the negative influence of suboptimal terminals on their satellite networks. Traditionally, SOTM testing is performed with actual operational satellites in field tests, which lack repeatability. The capability to repeat the conditions in which SOTM terminals are tested is important, especially when the performance of multiple terminals is compared. This contribution describes how the qualification test of SOTM terminals can be conducted in a laboratory environment so that repeatability can be ensured. A major advantage of a laboratory environment is the ability to test the complete terminal as if it was in the field of operation, yet without the involvement of real satellites effectively reducing the costs of testing. The main contributions of this paper are motion and shadowing profiles suitable for standardization of SOTM testing. Standardization of such profiles is necessary to guarantee a fair comparison of the performance of different terminals. Moreover, the paper presents the methodology for testing SOTM terminals at the Fraunhofer Facility for Over-the-air Research and Testing,* the procedure used to obtain the proposed profiles and results of testing a Ka-band SOTM terminal, taken as an example.

KEYWORDS

de-pointing, ESOG-120, GVF-105, on-the-move, satellite communications, testing

1 | INTRODUCTION

The Satcom on-the-move (SOTM) market has experienced a rapid growth in the recent years. A study for the European Space Agency in collaboration with the Global VSAT Forum (GVF) revealed that SOTM is seen by all members of the value chain as a primary source of new business.[1] In situations where no terrestrial communication infrastructure exists, SOTM systems represent one of the best solutions. Satcom on-the-move is a strong candidate in many other applications such as news gathering, mobile TV, public security, rescue, maritime, aeronautical, and military applications. However, SOTM systems still encounter many challenges, which hinder the potential market increase. Most challenging are antenna tracking and signal shadowing. The latter is often mitigated by forward error correction schemes.[2] The former not only causes a degradation in the link quality but is also a source of interference to adjacent satellites. This publication deals with SOTM broadband communication applications at Extremely High Frequencies (EHF). Although very small aperture terminals (VSATs) are desired to be used in SOTM systems due to their directive antennas and

*https://www.iis.fraunhofer.de/en/profil/standorte/forte.html

potential to provide high data rates, many satellite operators reported to be harmfully affected by VSAT interferences, eg, Rawlins.[3] To limit the interference caused by VSATs, regulatory authorities such as the International Telecommunication Union (ITU), the Federal Communications Commission (FCC), and the European Telecommunications Standards Institute (ETSI) define operational limits on the transmission from SOTM terminals.[4,5] In addition, the regulations specify limits on the maximum allowable pointing error of the SOTM antenna, the so-called *antenna de-pointing*, and define a transmit cessation time if the pointing error is larger than the permitted threshold.

Testing a SOTM terminal against these standardized limits is essential for the satellite operators in order to guarantee that the terminal does not cause harmful interferences to their satellite networks. Testing, moreover, offers SOTM manufacturers the ability to demonstrate the performance of their products and to identify their strengths and weaknesses. A comprehensive test that composes all the components of the SOTM terminal, including its outdoor unit and indoor unit, is necessary.

Antenna de-pointing, transmit cessation time, and Adjacent Satellite Interference (ASI) are measured to evaluate the tracking performance of the terminal. To evaluate the performance of the SOTM modem, channel emulators are used to generate realistic states of the communication link between the terminal and the satellite. The values of the free space path loss, the signal reception states (line of sight or blockage), the propagation delay, and Doppler are emulated as being in a real operational scenario. In this publication, the atmospheric losses, the rain attenuation, the Faraday rotation effect, etc, are not considered for analysis.

The existing state-of-the-art standards do not specify how the SOTM terminal is to be tested. Type approvals are operator specific and they, unlike standards, define the procedure in which the terminal should be tested. The core of all type approvals is similar and overlaps in the majority of the required tests. The GVF in its mutual recognition arrangement (MRA) working group initiated the GVF-105 document, which is agreed by the major satellite operators such as Eutelsat, Inmarsat, Intelsat, SES S.A. "A world leading satellite operator", and AsiaSat.[6] It includes recommendations for a mutually recognized testing procedure. In April 2017, GVF also published the Satellite Operator's Minimum Antenna Performance (SOMAP) requirements as a mutual agreement among the satellite operators on the minimum requirements, which SOTM terminals should meet.[7] Although all the standards define the metrics and the limits needed to test SOTM terminals, they do not specify under which environmental conditions the terminal shall be tested. For SOTM terminals, the conditions of the test environment are critical.

To ensure that their products are widely admitted and approved, terminal manufacturers need to run similar tests for the different satellite operators. This drives the costs and the time required for a terminal to be approved and increases the number of unauthorized terminals, which cause harmful interference to the different satellite networks. The development of a widely admitted standard for SOTM testing will give a basis for fair comparison compared with the potentially unfair evaluation of terminals based on their data sheets.

In a previous publication,[8] we proposed a methodology to test SOTM terminals in a laboratory environment in a controllable and repeatable manner under realistic conditions. In this contribution, we briefly review this methodology with a focus on the performance metrics which are defined in the SOTM standards and recommendations.

In Section 2, the state-of-the-art SOTM standards and recommendations are summarized and the state-of-the-art SOTM testing approaches are presented. In Section 3, the testing methodology is introduced. Section 4 discusses the process of developing the proposed standard motion profiles and their inclusion in the GVF-105 recommendations. In Section 5, the development process of the proposed standard shadowing profiles for the land mobile applications is presented. In Section 6, the results of the proposed testing procedures applied at the Fraunhofer Facility for Over-the-air Research and Testing (FORTE) are presented. The results highlight the advantages of testing the SOTM terminal based on the developed profiles.

2 | STATE-OF-THE-ART SOTM STANDARDS AND TESTING

At a global level, the ITU establishes standards which regulate the performance of all telecommunication platforms, including those relevant to SOTM. At the regional and the local levels, organizations such as the ETSI in Europe or the FCC in the United States adapt the general ITU regulations according to regional needs. Additionally, satellite operators issue type approvals to define how the SOTM terminals need to be tested. In this Section, an overview of the existing SOTM-related standards and type approvals is presented. Moreover, the state-of-the-art SOTM testing procedures are presented and compared.

2.1 | Satcom on-the-move standard metrics

The SOTM standards define operational limits with respect to the following metrics: antenna absolute de-pointing, off-axis emissions, and transmit cessation time.

The antenna absolute de-pointing is a measure in degrees that specifies how far the main beam of an antenna is displaced from a target satellite. The transmit cessation time and the off-axis emission specifications depend on this metric. Antenna de-pointing is the most important parameter, as it not only directly indicates the ability of the SOTM terminal to keep a high quality of the link towards the target satellite but also its ability to avoid ASI. The FCC regulations state that the antenna de-pointing should not exceed 0.2° at normal operating conditions in Ku-band. This limit can be raised to 0.5°, provided that in any case the transmit power does not exceed the regulatory EIRP Spectral Density (ESD) mask and that the value of the maximum de-pointing is reported to the satellite operator. For Ka-band, FCC does not specify an absolute de-pointing threshold. The pointing requirements are defined in terms of excess power levels. The ETSI norms require, for all frequencies, that the applicant specifies the value of the

maximum expected de-pointing as a function of on-axis ESD. The ESD mask must not be exceeded in any occasion. In the SOMAP requirements, the de-pointing threshold is specified at 0.5° for all frequency bands.[7]

The off-axis emissions are often parametrized by the transmit gain mask or the ESD mask. The gain/ESD mask defines the amount of gain/ESD allowed by the SOTM antenna as a function of the angular position relative the antenna boresight for co- and cross-polarized transmit components. The lower and the narrower the mask, the more challenging it is for the antenna to fulfill the off-axis emissions requirements. Different gain/ESD masks are defined by the different regulatory authorities depending on the application: commercial or military, and on the frequency of operation: Ku- or Ka-band. In general, the commercial Ka-band masks are narrower and more stringent than the commercial Ku-band masks.[9] The military Ka orbit/band is not yet crowded, the MIL-STD-188-164B Ka-band mask, defined by the Department of Defense, is therefore the most flexible among all. As an example for a regulatory mask specified in SOTM recommendations, the GVF-SOMAP requirements adopt the gain mask named the $'32 - 25\log(\theta)'$ [dBi] mask for the Ku-band and the gain mask $'29 - 25\log(\theta)'$ [dBi] for the Ka-band.

The transmit cessation time, also referred to as the transmit mute time, is defined as the time period that the SOTM terminal stays active before it switches off its transmit activity if the antenna de-pointing is larger than a specific threshold. The FCC Blanket Licensing Provisions §25.226 and the §25.222 define the transmit mute time to be 100 ms if the antenna de-pointing exceeds 0.5°.[4] The GVF-SOMAP requirements adopt the same definition. The ETSI regulations leave the exact definition of this metric to the applicant but state that it should not exceed 2 seconds in case on Vehicle Mounted Earth Stations[5] or 5 seconds for Earth Stations on Vessels.[10]

Table 1 lists the state-of-the-art SOTM standards, regulations, and norms for each environment: land mobile, maritime, airborne, and railway for the Ku and Ka frequency bands.

TABLE 1 The state-of-the-art SOTM standards, regulations, and norms listed for each environment and each frequency band

	Land Mobile		Maritime		Airborne		Railway	
	Ku	Ka	Ku	Ka	Ku	Ka	Ku	Ka
ITU	R 728-1	R S.524	R 728-1	R S.524	R 728-1	R S.524	R 728-1	R S.524
	R S580-6	R S580-6	R S580-6	R S580-6	R S580-6	R S580-6	R S580-6	R S580-6
	R S.1875	R S.1875	R S.1875	R S.1875	R S.1875	R S.1875	R S.1875	R S.1875
FCC	p25.226	p25.138	p25.222	p25.138	…	p25.138	…	p25.138
DoD	MIL-STD-	MIL-STD-	MIL-STD-	MIL-STD-	MIL-STD-	MIL-STD-	…	…
	188-164B	188-164B	188-164B	188-164B	188-164B	188-164B		
	Ku-Section A	Ka-Section A	Ku-Section C	Ka-Section C	Ku-Section B	Ka-Section B	…	…
ETSI	EN 302 977	EN 303 978	EN 302 340	EN 303 978	EN 302 186	EN 303 978	EN 302 448	EN 303 978
GVF	SOMAP	SOMAP	SOMAP	SOMAP	SOMAP	SOMAP	SOMAP	SOMAP

Abbreviations: DoD, Department of Defense; ETSI, European Telecommunications Standards Institute; FCC, Federal Communications Commission; GVF, Global VSAT Forum; ITU, International Telecommunication Union; SOMAP, Satellite OperatorŠs Minimum Antenna Performance; SOTM, Satcom on-the-move.

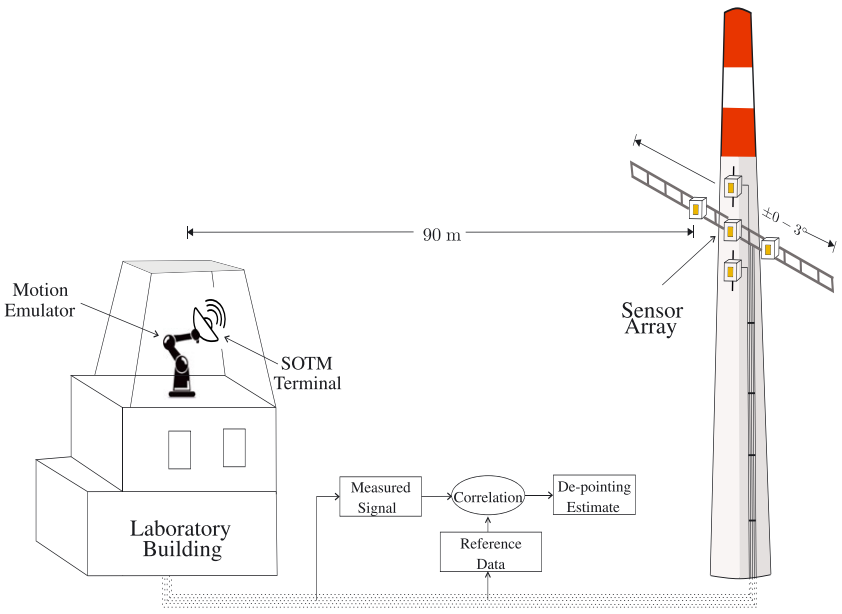

FIGURE 1 De-pointing measurements at the Fraunhofer Facility for Over-the-air Research and Testing. SOTM, Satcom on-the-move [Colour figure can be viewed at wileyonlinelibrary.com]

2.2 | Testing procedures and environments

The majority of the existing laboratories has the ability to test only parts of the SOTM terminal. The authors are aware of only two facilities, which are built to test the complete SOTM terminal: the Aberdeen Proving Ground in Maryland, USA, and the FORTE in Ilmenau, Germany. Due to the dimensions of the laboratory at Aberdeen Proving Ground, tests are performed in the near field of the antenna.[11] The beam of the antenna will be spread depending on how far in the near field the antenna is operating.[12] Fraunhofer Facility for Over-the-air Research and Testing performs SOTM testing of the complete terminal in the far field in a repeatable and controllable way. The emulation of the realistic environment, a SOTM terminal would experience, is possible by the usage of satellite payload emulators, a three-axis motion emulator, channel, and GPS emulators. A two-dimensional sensor cross mounted on an antenna tower (cf Figure 1) enables the estimation of antenna de-pointing with high precision. A description of FORTE with detailed technical parameters can be found in Siegert et al. [13]

3 | PROPOSED TESTING METHODOLOGY

This section presents the methodology we propose to perform qualification tests of SOTM terminals at FORTE. The terminal is tested with respect to the standard performance metrics discussed in Section 2.1. Furthermore, we define the *data traffic throughput* as a metric to test the performance of the modem under realistic conditions.

In a first step of the SOTM qualification test, the antenna pattern is measured. At FORTE, with a distance of 90 m between the terminal and the antenna tower (cf Figure 1), a far field distance for antennas with a diameter up to 90 cm in the Ku-band and up to 70 cm in the Ka-band is ensured. In the commonly used setting, the motion emulator is used to rotate the antenna for pattern measurements. The used motion emulator ensures a high degree of position accuracy (approximately equal to 0.05 arc sec). The center sensor on the antenna tower works as a probe and is used for pattern measurements.

3.1 | Off-axis emissions measurements

For the evaluation of the off-axis emissions, the difference between the far field gain pattern and regulatory gain/ESD mask is calculated. In case there are angular positions at which the pattern exceeds the mask, they are reported together with the corresponding levels. This test evaluates the performance of the SOTM antenna and the block up converter at once. If the measured pattern violates the regulations, the manufacturer needs to redesign the antenna in order to reshape the main lobe or one of the side lobes. Alternatively, either the amount of power transmitted by the block up converter can be reduced to match the ESD mask, or the spectrum spreading techniques are applied. However, this leads to a degradation of the overall quality of the communication link.

3.2 | Antenna de-pointing measurements

To measure the antenna de-pointing, the motion emulator plays back a motion profile. Hence, the SOTM antenna experiences a de-pointing, which it tries to compensate using its foreseen mechanisms. The remaining de-pointing error, due to imperfect compensation is detected by a sensor array mounted on the antenna tower as shown in Figure 1. Therefore, if the terminal is tested under the effect of motion only, and the effects of other impairments such as signal shadowing and Doppler are disabled, the proposed method for the antenna de-pointing measurements explicitly shows how good the tracking unit performs.

While the SOTM antenna is being on-the-move and transmitting, the sensor array is detecting the received power at five spatial points (cross-shape).

The description of the de-pointing estimation algorithm developed by the authors was introduced in Alazab et al.[8]

The azimuth sensors can be adjusted in an angular range of $\pm 0 - 3^{\circ}$. This enables an adaptation according to the shape of the antenna pattern, which is important to achieve the highest possible antenna de-pointing estimation precision that is possible for a given 3-dB beam width of the antenna. In Alazab et al,[8] the optimum sensor positions as a function of the antenna 3-dB beam width was inspected. It was shown that the de-pointing estimation accuracy can reach 0.005° on some synthetic sinusoidal motion tracks.

In contrast to tests in a free field range, this framework allows to measure the antenna de-pointing both in azimuth and elevation. Furthermore, it enables a more accurate de-pointing estimation.

For electrically steerable antennas and phased arrays with beam patterns that change depending on the steering direction, ASI can be used to judge the pointing performance. At FORTE, ASI can be measured by adjusting the positions of the outer azimuth sensors on the tower at the places where the adjacent satellites are located. Another extension of the sensor array that is based on increasing the number of sensors will allow to estimate the main beam and the first side lobes of the phased array while the terminal is on-the-move. This extension will be considered in the future and is not in the scope of this contribution.

As a part of an example type approval, the de-pointing estimation results of a SOTM dish antenna are presented in Section 6.

3.3 | Transmit mute measurements

To be compliant with the regulations, it is compulsory that any SOTM terminal be fitted with a mute functionality. It inhibits transmissions when either of the two following conditions is met:

- The antenna de-pointing exceeds the regulatory threshold, eg, 0.4° for EUTELSAT. This information must be delivered by the antenna control unit (ACU).
- The modem loses synchronization of the out-route.

The SOTM terminal switches off the transmit signal either using the ACU or the modem. The delay time before the signal is switched off or attenuated when the antenna de-pointing exceeds the regulatory threshold is measured. As per FCC and GVF regulations, the transmit mute delay should not exceed 100 ms if the de-pointing exceeds 0.5°. The ACU must not switch on the transmit signal again unless the de-pointing is reduced to 0.2° or less. The accurate measurement of the antenna de-pointing, as illustrated in Section 3.2, ensures the accurate evaluation of the transmit mute functionality of the SOTM terminal.

3.4 | Data traffic measurements

Monitoring the data traffic flow is important to evaluate the overall performance of the SOTM terminal also including the modem. The SOTM modem should be able to adapt the modulation and coding schemes depending on the channel status and on the network topology. Different network topologies, eg, star or mesh topology can be applied in the test. The data traffic flow is evaluated at the different nodes in the network. At FORTE, the data traffic can be evaluated with respect to all relevant parameters (Doppler, shadowing, motion, etc) at once or separately for a selected parameter.

4 | PROPOSED MOTION PROFILES

An essential part of the performance tests, described in Section 3, depends on the proper choice of the motion profile. In Alazab et al,[1] the data sheets of 100 SOTM terminals were investigated including the most popular and widely deployed ones nowadays. Out of this representative sample group, only 8% mentioned the motion profile used to test the terminal. For the remaining 92%, either no motion track is specified or no information about testing is mentioned at all. This complicates the comparison of SOTM terminals from the different vendors. An objectively compared poor performing SOTM terminal may outperform a good one simply because of the choice of a motion profile that leads to an unfair comparison. Therefore, to standardize motion profiles is important to provide a fair judgment and comparison of SOTM terminals. A framework to select representative motion profiles and propose them as a standard is one of the major contributions of this paper.

In this section, the procedure to define the proposed motion profiles is introduced. Additionally, motion profiles are defined for the land mobile and the maritime environments. An extension including the aeronautical and the train environments is planned for the future.

In general, four steps have been considered in order to develop the motion profiles:

1. Measurement of the motion dynamics.
2. Statistical analysis: The complete manifold of measurements has been segmented. A *measurement segment* is defined as the motion dynamics, eg, angular positions or rates, over a certain period of time. Statistical measures like the mean and the variance have been then extracted from each measurement segment.
3. Measurement classification: The measurements were classified in two classes based on the extracted statistics. The classes have been labeled, namely, Classes A and B.
4. Profile selection: A representative motion profile for each class has been selected and proposed as a standard motion profile for the corresponding class.

In the following, each of the four steps is described in more detail.

4.1 | Measurement of the motion dynamics

In the context of an European Space Agency project,[14] multiple measurement campaigns were performed in the land mobile and maritime environments. The measurement campaigns were carefully planned in order to

- cover the largest possible variety of measurement scenarios in each environment. A *measurement scenario* is specified by its environment type, its terrain type, and its platform type.
    - Environment type: land mobile or maritime.
    - Terrain type: for each environment, different terrain types were considered. For example, off-road or highway in the land mobile environment, and storm or rough sea in the maritime environment.

- Platform type: the platform is the vehicle which is used to measure the motion dynamics, eg, pickup or bus in the land mobile environment, and large vessel or small rescue boat in the maritime environment.

- include well known or reference test tracks if possible. For example, measurements were performed at the Millbrook Proving Ground in the UK. The tracks at the Millbrook Proving Ground include a variety of terrain types such as off-roads with deep ditches, federal ways with ramps, and special tracks with sinusoidal surfaces.

A high precision in measuring the motion dynamics was guaranteed by using an inertial measurement unit (IMU), which employs fiber optic gyroscopes. The measured dynamics include angular positions, rates, and accelerations as well as translational velocities and accelerations. These parameters were measured for each of the three body axes: yaw, pitch, and roll. A measurement database was created including a total of 33-hour-long maritime and 30-hour-long land mobile measurements. [15]

4.2 | Statistical analysis

The analysis of the motion dynamics is based on statistical parameters. For each measurement segment, the minimum, maximum, mean, and standard deviation of the measured dynamics were extracted. The probability density function (PDF) and the cumulative distribution function (CDF) were also calculated.

The parameter space is multidimensional. To facilitate the definition of the motion profiles, a single parameter should be selected. The 95% quantile of the measured angular rate vector norm is selected.[14] The vector norm of the angular rate of the yaw, pitch, and roll axes is calculated as in Equation 1.

$$Rate_{\text{norm}} = \sqrt{Rate_{\text{yaw}}^2 + Rate_{\text{pitch}}^2 + Rate_{\text{roll}}^2} \tag{1}$$

4.3 | Measurement classification

Satcom on-the-move applications can be seen as divided in two main classes: applications in harsh conditions such as in military or in disaster scenarios, and applications in smoother motion conditions such as mobile internet backhauling. A threshold to classify the measurements according to these two classes is defined based on the distribution of the Q95 values of the angular rate vector norm as will be explained in Section 4.5 in detail.

4.4 | Profile selection

A representative motion profile is selected for each class. The mean and the confidence interval (standard deviation) of the Q95 angular rate vector norm values of each class were calculated, and the measurement segment with the closest value to the mean is chosen as the representative motion profile of the corresponding class. The profiles are proposed as a standard to be used for testing the different types of SOTM terminals.

4.5 | Applying the procedure for land mobile and maritime

The four steps of the standard motion profile definition process were applied for the land mobile and the maritime environments. Because of the size limitations of this contribution, the process will be presented for the land mobile environment only.

Five platforms and seven terrain types were included in the land mobile measurement campaign. Table 2 shows how the terrain types were covered by the different platforms. For example, the bus was used only on rural, urban, and highway terrains.

In Figure 2, the Q95 angular rate vector norm values are plotted in a scatter plot versus terrain type. Each point represents the Q95 angular rate vector norm of one measurement segment of one terrain measured with each of the given platforms represented by the different markers. The measurements collected at Millbrook are plotted using a different marker, the black diamonds.

The PDF of the Q95 angular rate vector norm values is depicted in Figure 3.

From Figure 3, it can be seen that the distribution has three modes and a tail. The two measurement classes were defined based on this shape. Class A that represents harsh terrains and off-roads will include all measurements in the tail of the PDF. Class B that represents paved terrains

TABLE 2 Platforms and terrain types used in the land mobile measurement campaign

	Off-road	Gravel	Mixture	Rural	Urban	Federal	Highway
Pickup	x	x	x	x	x	x	x
Truck	x	x		x	x	x	x
Small van	x	x	x	x	x	x	x
Bus				x	x		x
Passenger car			x				

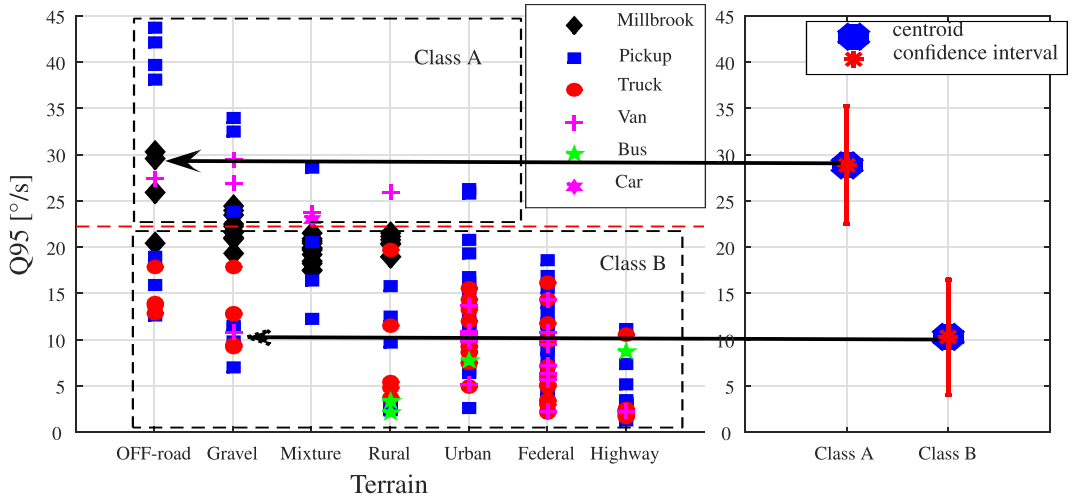

FIGURE 2 Motion profile selection process for the land mobile environment. In the left subfigure, the Q95 values of the angular rate vector norm are shown. In the right subfigure, the mean and confidence interval of the Q95 angular rate vector norms are depicted. The measurement closest to the mean value is selected and proposed as a standard motion profile. The Class A profile is an off-road Millbrook measurement with a pickup, while the Class B profile is a gravel dirt road measurement with a van [Colour figure can be viewed at wileyonlinelibrary.com]

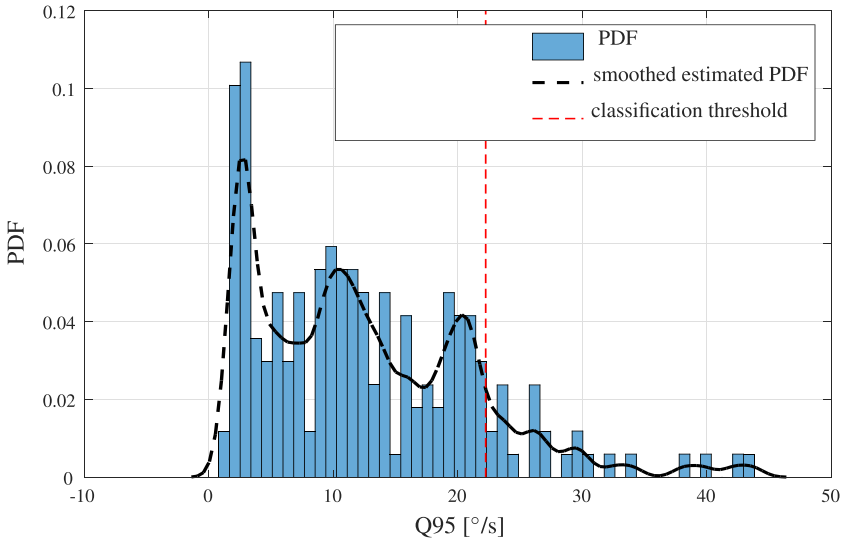

FIGURE 3 The PDF and its smoothed estimation of the Q95 values of the angular rate vector norm for the land mobile environment. A threshold defined at 22.24°/s (red dashed line) separates Class A that represents harsh terrains from Class B, which represents paved terrains [Colour figure can be viewed at wileyonlinelibrary.com]

and relaxed off-roads will include all measurements in the three modes. The separation threshold is defined at the falling edge of the third mode at 22.24°/s. This value divides 10% of the measurements to be belonging to Class A and 90% to be belonging to Class B.

The threshold level is also shown in the left subfigure of Figure 2, and the two classes are also labeled.

The right subfigure of Figure 2, depicts the mean and the standard deviation values of all measurements in each class.

The proposed standard motion profiles selection is depicted in Figure 2. The black arrows point at the measurement segments, which are selected for Classes A and B. The representative profiles have a Q95 of the angular rate vector norm that is closest to the mean for each class. For the land mobile Class A, the representative motion profile is an 8 minutes measurement segment on a off-road at Millbrook with the landrover as the platform. For Class B, the representative motion profile is another 8 minutes segment on gravel dirt road driven with the van.

The same process was applied for the maritime environment. The maritime Class A proposed standard motion profile is selected as a 15 minutes measurement segment in moderate sea conditions with a rescue boat from the Royal Netherlands Sea Rescue Institution (KNRM). The Class B profile is a 15 minutes measurement with the same rescue boat in calm sea conditions.

Figure 4 depicts the CDF of the angular rate vector norm for the Classes A and B representative motion profiles of the land mobile and the maritime environments. The CDF of the angular rate vector norm for the Churchville B motion track is plotted in the same figure for the sake of comparison. The dynamics of the Churchville B track are very close to the dynamics of the land mobile Class B representative motion profile.

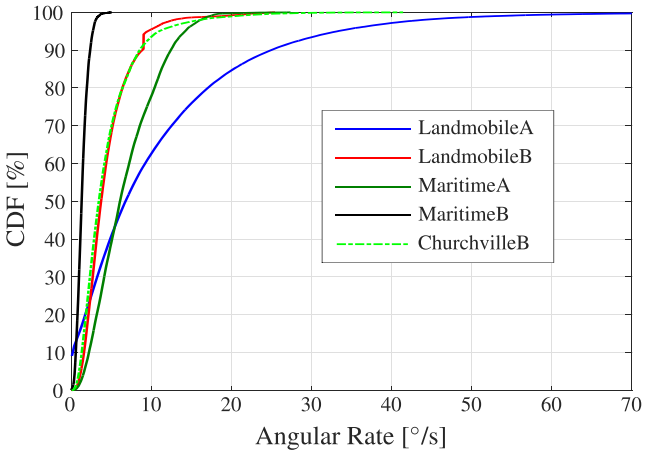

FIGURE 4 The CDF of the angular rate vector norms for the motion profiles of Classes A and B of the land mobile and the maritime environments. The CDF of the angular rate vector norm for the Churchville B motion track is also plotted. CDF, cumulative distribution function [Colour figure can be viewed at wileyonlinelibrary.com]

It can be seen from Figure 4 that the land mobile Class A represents the upper bound of the motion dynamics and the maritime Class B represents the lower bound.

4.6 | Proposed motion profiles in GVF-105

The authors of this paper developed the motion profiles described in this section and proposed them to GVF-MRA working group, which showed a great will to apply them in their future testing plans. As a result, the motion profiles were added to the GVF-105 document. It is stated as a recommendation that a SOTM terminal is to be tested using the proposed profiles in either

- A laboratory environment where the dynamics and the actual time series of the motion profiles from Classes A and B can be replayed and the tracking performance can be measured, or
- A free field: In this case, it has to be ensured that at least the statistics of the test track match the statistics of the selected representative motion profiles for the corresponding environment and class. It also has to be ensured that an accurate IMU is used to record the dynamics of the motion profile during the test such that the dynamics can be compared.

5 | PROPOSED SHADOWING PROFILES

The channel between the SOTM terminal and the target satellite is often referred to as the land mobile to satellite (LMS) channel. The line-of-sight (LOS) and nonline-of-sight (NLOS) conditions of the LMS channel depend on the environment around the SOTM terminal and on the pointing direction to the satellite. The LOS and NLOS effects (also called shadowing effects) need to be considered when the SOTM terminal is tested.

Land mobile to satellite channel characterization, so far, depends on statistical modeling or on RF measurements. The statistical channel models, eg, those proposed in other works,[16-18] derive the time series of the channel states using parameters driven from statistical distributions. For the Ku-/Ka-band frequencies that are relevant for the scope of this paper, there exist no statistical model in the literature, which is able to model the LMS channel at these high frequencies for any satellite position and any environment scenario. There exist some models based on RF measurements at Ku-/Ka-bands, eg, Scalise et al[19] and Kubista et al,[20] however, they are only valid for limited positions of satellites and limited number of environments. The characteristics of the Ku-/Ka-band satellite channel (11-40 GHz) are similar to those of the optical channel. Multipath components are irrelevant and can be neglected since SOTM applications usually use directive antennas.[21] With respect to the shadowing, the Ku-/Ka-band LMS channel can be treated as a frequency-flat ON/OFF channel. Based on this observation, we propose standard shadowing profiles in this section based on the processing of optical images.

The proposed standard shadowing profiles offer a unique reference or a benchmark for SOTM terminal testing and comparison. They can be used in any laboratory, which employs channel emulators. If the terminal is tested in a field test instead, it is recommended that the shadowing profile from the field test track statistically matches the developed shadowing profiles presented in this section. This maintains a fair basis to test and compare different SOTM terminals.

To define the shadowing profiles, four steps are involved. These are the following:

1. Image capturing and environment definition.
2. Image post processing: classification of the images into LOS or NLOS.

(A) An exemplary hemispheric image from an urban environment.

(B) An overlay consisting of the original and the binary categorization into *sky* and *obstruction*.

FIGURE 5 The original hemispheric image (left) and the result of the image classification (right) [Colour figure can be viewed at wileyonlinelibrary.com]

3. Shadowing profile extraction: profile extraction from the processed images at a certain angular position.
4. Selection of proposed standard shadowing profiles: one shadowing profile for each environment is selected as a representative shadowing profile.

In the following, these steps are presented in detail.

5.1 | Image capturing and environment definition

In addition to the measurement of the motion dynamics described in Section 4.1, a fisheye camera pointing towards the sky was mounted on the rooftop of the vehicles. A sequence of images of the upper hemisphere were captured at a rate of five frames per second along a specific motion profile. We denote this sequence as "image profile." As an example, Figure 5A shows a single snapshot of a hemispheric image profile in an urban scenario.

The image profiles were classified into seven different environment types: forest, urban, suburban, light tree shadowed, highway, open, and train.

5.2 | Image post processing

A classification algorithm segregates the image into regions with LOS and NLOS.[22] The algorithms filters the sun spot and the clouds in order to exclude their effects. Figure 5B shows the two classes for the same snapshot depicted in Figure 5A. Red represents NLOS or obstruction while blue represents LOS or sky.

For a better representation of azimuth and elevation angle pairs, the image is transformed into a rectangular landscape panoramic monochrome format. The new angular grid has a resolution of one degree in both, azimuth and elevation. This transformation is followed by a circular rotation in azimuth to account for heading compensation. The image is rotated by the vehicles heading, such that the resulting image will have the geographical north at 0° in azimuth.

5.3 | Shadowing profile extraction

Knowing the geographical location, ie, the longitude and latitude of the vehicle at a specific time, the location (azimuth and elevation) of a specific satellite, given its orbital longitudinal position, can be determined. Based on the obtained azimuth and elevation angle pair, the reception state of the satellite can be extracted from the panoramic image. The shadowing profile related to one motion profile can be generated by extracting the LOS information from the sequence of images in the corresponding image profile. Figure 6 shows an exemplary monochrome panoramic image profile with azimuth, elevation, and time. Figure 7 depicts the shadowing profile corresponding to the land mobile Class A proposed standard motion profile if the EUTELSAT 10A satellite located at 10° East is considered. The profile consists of two shadowing levels, "ON" for no shadowing (LOS) and "OFF" for obstruction (NLOS). The percentage of LOS for the land mobile Class A corresponding shadowing profile is approximately 94%.

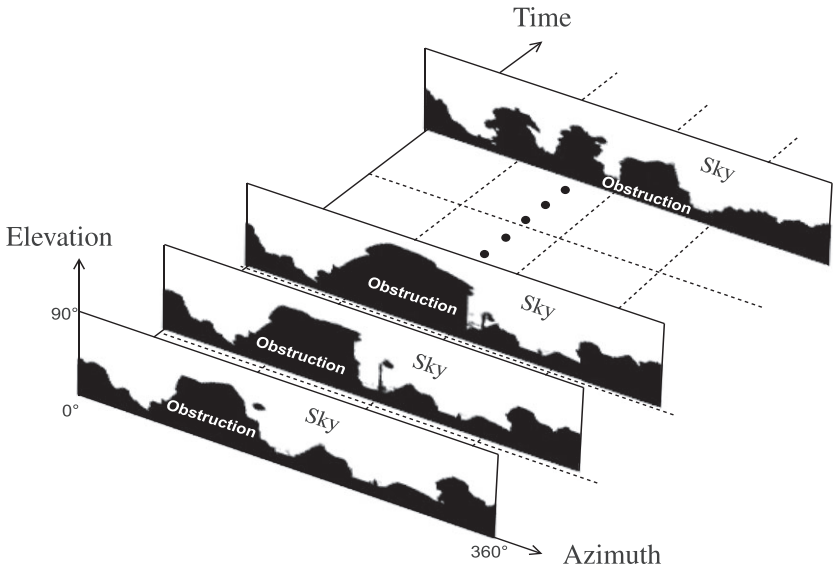

FIGURE 6 An exemplary panoramic image profile showing the line-of-sight and nonline-of-sight reception states for each azimuth and elevation angle pair at each time instance. The image capturing rate defines the number of images in the whole duration of the profile

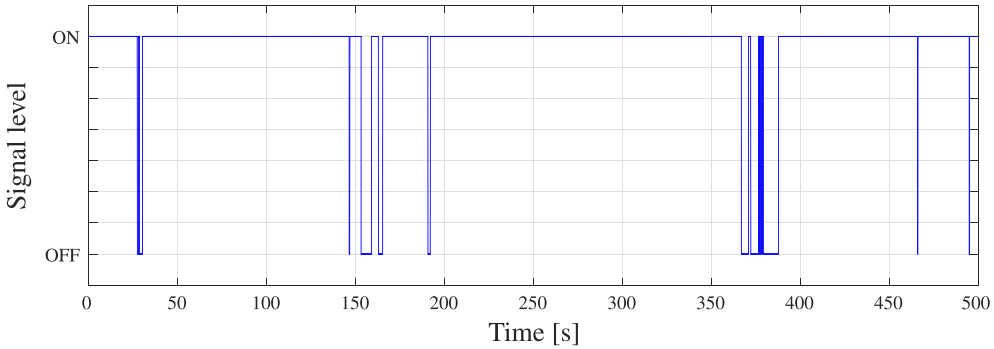

FIGURE 7 The shadowing profile extracted from the image profile captured at the Class A motion profile for the EUTELSAT 10A satellite. ON represents no shadowing (line-of-sight [LOS]) and OFF represents obstruction (nonline-of-sight). Approximately 94% of the profile is covered by LOS [Colour figure can be viewed at wileyonlinelibrary.com]

Using this image-based method, shadowing profiles for different satellite positions can be obtained. In a field test, in contrast, this is not possible unless the complete measurement is repeated for each satellite position or if multiple antennas are involved in the measurement, each pointing towards a different satellite.

5.4 | Definition of shadowing profiles

To select and define the shadowing profiles, we consider the "percentage of LOS in the shadowing profile." For each azimuth and elevation angle pair in every image profile, a shadowing profile (cf Figure 7) is extracted, and the percentage of LOS is calculated along time dimension. For the sake of simplicity, the dimensions are further reduced by averaging the LOS percentage over all azimuth angles. This results in the mean LOS percentage versus elevation and is denoted the "LOS-elevation contour."

Additionally, the mean of all LOS-elevation contours is calculated for each environment. The resulting mean is denoted as the "environment mean LOS-elevation contour" and is depicted for each of the defined environments in Figure 8.

In a next step, the root-mean-square deviation between the individual LOS-elevation contours and the corresponding environment mean LOS-elevation contour (cf Figure 8) is calculated. For each environment, the image profile with the lowest root-mean-square deviation is selected as the proposed standard image profile. For a specific satellite location, the proposed standard shadowing profile is then extracted from the standard image profile.

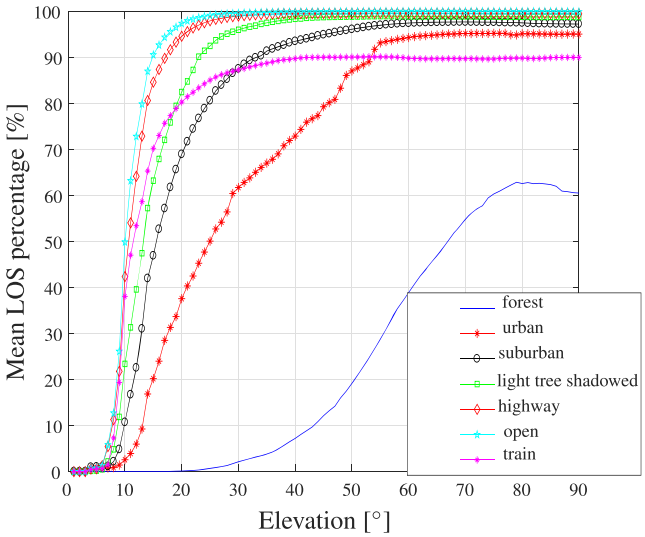

FIGURE 8 The environment mean line-of-sight (LOS)-elevation contours for the seven defined environments [Colour figure can be viewed at wileyonlinelibrary.com]

5.5 | Combining the motion profiles and the shadowing profiles for testing

In a SOTM terminal test scenario, the shadowing profile should always be synchronized to the corresponding motion profile. However, the combination of a shadowing profile from one geographical location with a motion profile from a different geographical location is needed for a SOTM terminal test in a laboratory environment, such as FORTE. This is important in order to test the performance of the SOTM terminals with different combinations of motion and shadowing. Here, three main challenges exist:

1. The heading in the image profile does not match the heading in the new motion profile, which is from a different location.
2. The image profile and the new motion profile may not have the same length in time.
3. The speed of the vehicle while capturing the image profiles does not match the speed of the vehicle at the motion profile.

The definition of the motion profiles (cf Section 4.2) is based on the vector norm of the angular rates. To investigate if the heading mismatch between the image and the motion profiles needs to be compensated or can be neglected, the correlation between the gradient of the heading, and the gradient of the roll and pitch angles was investigated. If the correlation is low, the evolution of the heading in the image profile is considered independent of the evolution of the dynamics in the motion profile and no heading compensation is required.

It has been found that the correlation coefficient does not exceed 0.25 in any case. Hence, the heading from the image profile does not need to match the heading in the motion profile. In other words, the image profile can be used with its original heading to extract the shadowing profile at any geographical location on earth.

To overcome the second challenge, which is to match the length of the image profile to the length of the motion profile, two cases need to be considered:

1. The image profile is longer than the motion profile: we choose the part of the image profile which yields a shadowing profile having a LOS percentage, which is closest to the one expected from Figure 8 for the corresponding satellite elevation.
2. The image profile is shorter than the motion profile: we flip and repeat the image profile multiple times, and fill the last segment with the part of the image profile, which guarantees the closest LOS percentage to the one expected from Figure 8 for the corresponding satellite elevation.

The third challenge, which is the different speeds of the vehicle at the shadowing and motion profiles, can be overcome by stretching or shrinking the LOS/NLOS states in the shadowing profile. For instance, if the average speed at the motion profile is double the average speed at the shadowing profile, the shadowing profile will be down-sampled by rate of one-half. Afterwards, the new down-sampled profile will be repeated twice in order to keep the same original length and LOS/NLOS statistics. For the sake of simplicity, we assume that the motion profiles and the image profiles are driven at the same speed for the rest of the analysis.

The proposed standard shadowing profiles for the defined seven environments extracted at the geographical location of the land mobile Class A motion profile for the EUTELSAT 10A satellite are depicted in Figure 9.

Generally, the motion of the vehicle causes Doppler, ie, frequency shifts inside the band of operation occur. Investigations of Doppler effects are not considered in this contribution. In measurements performed at FORTE, we experienced that the effect of Doppler on the overall performance of the SOTM terminal is marginal compared with the effect of the motion or of the shadowing. It is more challenging for the modem to mitigate the effect of signal blockages than to handle frequency shifts caused by the Doppler effect. Moreover, other impairments, eg, the atmospheric losses, the rain attenuation, and the Faraday rotation effect, are not considered in this contribution.

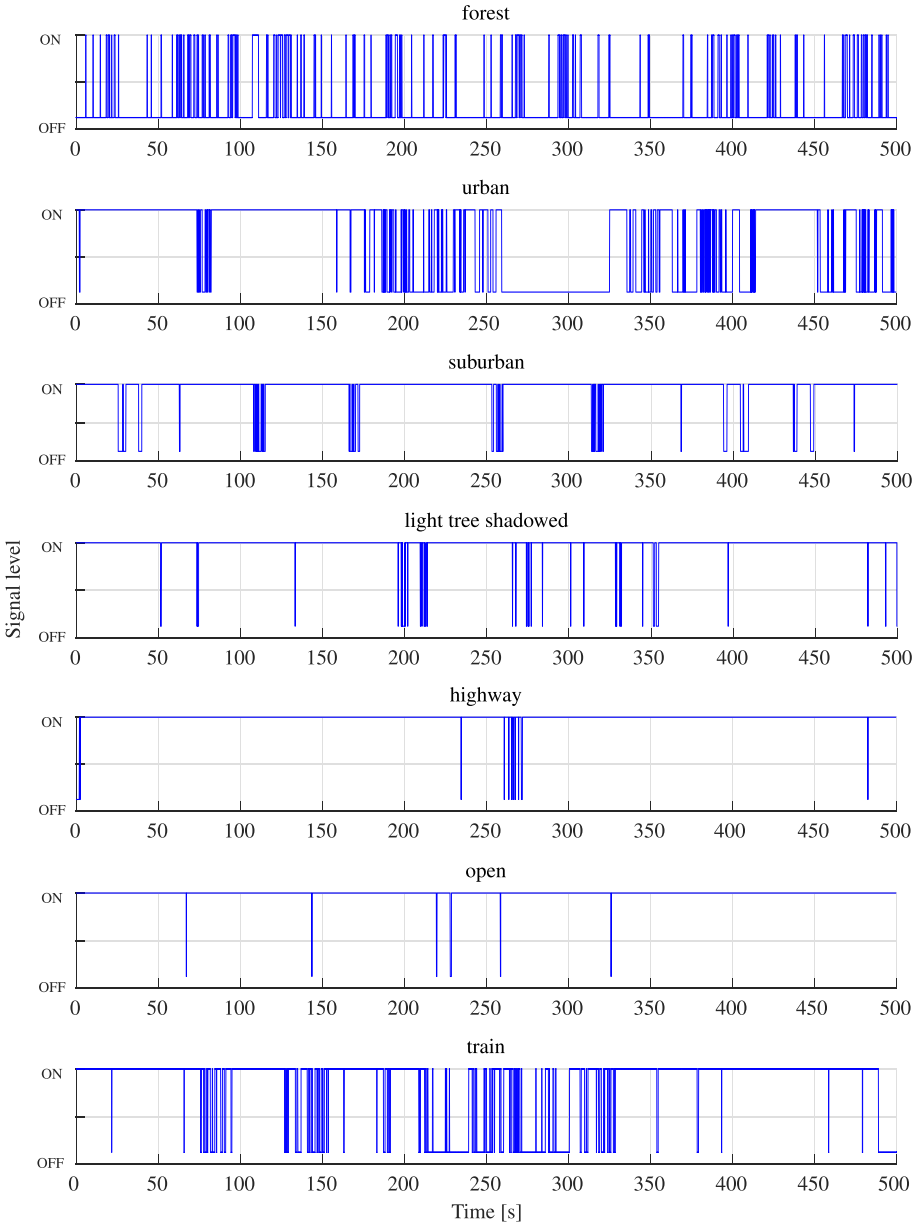

FIGURE 9 The proposed standard shadowing profiles for the different environments assuming the geographical location of the land mobile Class A motion profile and the EUTELSAT 10A satellite located at 10° East [Colour figure can be viewed at wileyonlinelibrary.com]

6 | MEASUREMENT RESULTS

In this section, the results of a tested Ka-band SOTM antenna at FORTE are presented. The test was performed in compliance with the type approval recommendations (GVF-105) defined by the GVF. As the GVF-105 recommendations do not specify operational limits, the specifications ESOG-120[23] and the EESS-502[24] from EUTELSAT were applied additionally.

6.1 | The measurement scenario

The antenna under test and its tracking unit were developed in the context of the project KASYMOSA (Ka-Band Systems for Mobile Satellite Communications).† This project aimed to develop and validate new technologies and algorithms for mobile satellite communications in the Ka-band. The developed antenna has a dish with a diameter of 60 cm and operates in the Ka-band (approximately equal to 30 GHz uplink and approximately equal to 20 GHz downlink). A mechanical two-axis tracking unit is attached to the antenna in order to track in azimuth and elevation.[25]

†The project KASYMOSA was supported by the German Aerospace Center (DLR).

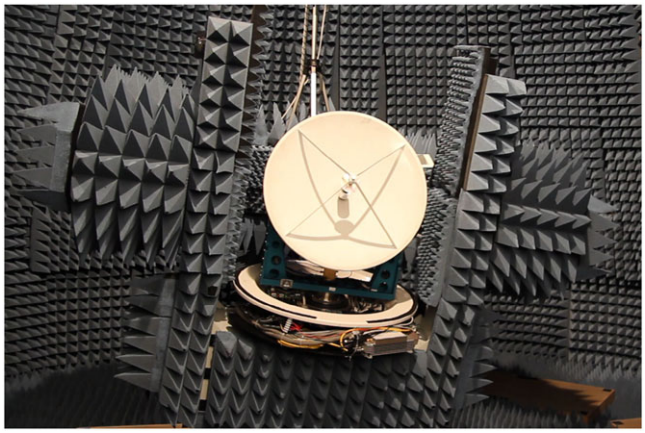

FIGURE 10 The antenna under test while being mounted on the motion emulator and tested at Facility for Over-the-air Research and Testing [Colour figure can be viewed at wileyonlinelibrary.com]

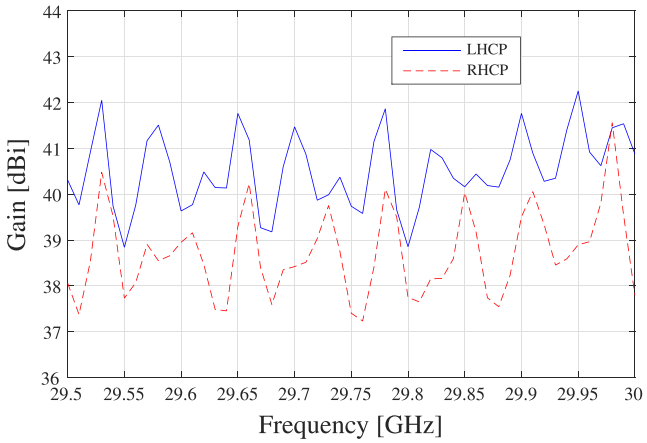

FIGURE 11 The transmit co-polarized gain of the antenna under test vs frequency for both polarizations left-hand circular polarization (LHCP) and right-hand circularly polarized (RHCP) [Colour figure can be viewed at wileyonlinelibrary.com]

An attached IMU measures the orientation of the SOTM terminal. The heading information is estimated with the help of GPS. A phase discriminator gives an initial indication of the pointing error by evaluation of the received beacon from the satellite. Finally, the collected data are fed into a control algorithm based on Kalman filtering in order to perform successful satellite tracking.

A picture of the antenna mounted on the motion emulator at FORTE is shown in Figure 10.

6.2 | An excerpt of the SOTM type approval results

The tests performed at FORTE include the following:

- Antenna characteristics: This includes the measurements of antenna transmit and receive gains, and patterns at the different required frequencies, polarizations, elevation pre-tilts, and radome orientations.
- Dynamic tests: This includes the measurements while the antenna is moving on the proposed standard motion profiles. Antenna de-pointing, cross-polarization discrimination (XPD), ASI are measured.

6.2.1 | Antenna characteristics

6.2.2 | Gain measurements

The antenna gain is measured as a first step. This measurement is performed directly at the feed port of the antenna. During the measurements, a single tone is transmitted by the antenna under test and the power level at the receive antenna at the antenna tower is recorded. The antenna gain (in main beam direction) is finally obtained by comparison with a reference antenna with known gain. Repeating this for multiple frequencies and both polarizations (left-hand circular polarization [LHCP] and right-hand circularly polarized) results in the main beam antenna gain provided in Figure 11.

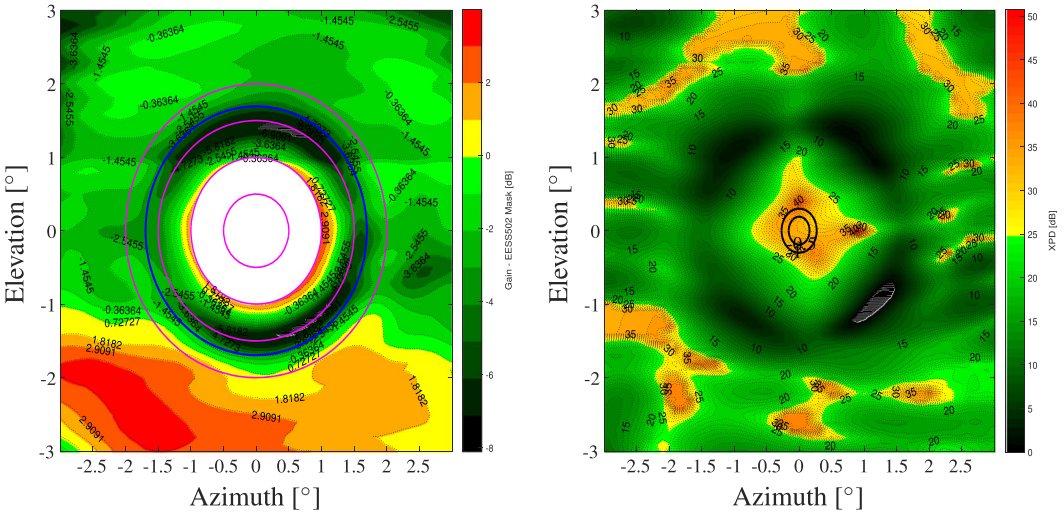

(A) Transmit co-polar raster scan - $'29 - 25\log(\theta)'$ overshoots from 1° for antenna elevation 30°, frequency 29.5 GHz, and LHCP polarization. The measured pattern does not fulfill the requirements of EUTELSAT.

(B) Transmit XPD raster scan with the -0.5 dB and -1 dB templates for antenna elevation 30°, frequency 29.5 GHz, and LHCP polarization.

FIGURE 12 Raster scans of transmit co-polar overshoots and cross-polarization discrimination (XPD). LHCP, left-hand circular polarization [Colour figure can be viewed at wileyonlinelibrary.com]

6.2.3 | Radiation pattern measurements

The motion emulator is used to move the antenna in order to measure its patterns in the transmit and receive frequency bands. The EUTELSAT specifications[23] require measuring the antenna gain patterns at multiple antenna elevation pre-tilt angles. Hence, at least two elevations need to be measured: 0° and one angle between 30° and 35°. The specifications also require measuring the patterns at the center frequency and two other frequency points one in the lower half and one in the upper half of the transmit frequency band. For example, for the Ka-band uplink, the frequencies 29.5, 29.75, and 30 GHz need to be considered. A further requirement is to measure the pattern while having multiple radome rotations: 0°, 90°, 150°, and 270°. This makes the measurement manifold multidimensional. For the sake of brevity, we only render an excerpt of the results in this section.

The EUTELSAT specifications require that the antenna gain pattern at the transmit frequency bands has to be in conformance with the $'29 - 25\log(\theta)'$ mask. The measured radiation pattern is plotted along with the mask and the conformance is investigated. In Figure 12A, the mask overshoots are plotted for a single measurement scenario. The mask overshoot is the difference between the gain pattern and the regulatory mask. The colors of the plot represent an overshoot/no-overshoot schema. Green and black represent no overshoot, while yellow and red represent regions with overshoots. The depicted measurement is at an uplink frequency of 29.5 GHz, LHCP polarization and an antenna elevation of 30° while the radome was put off.

According to the specifications, the plot starts at 1° deviation from the main beam direction. Hence the inner circle is not measured. The magenta circles highlight contours with 0.5° angular difference, whereas the blue circle represents the α angle specified by EUTELSAT. $\alpha = 1°$ or $100\lambda/D$ whichever is greater, where D is the antenna diameter and λ is the carrier wavelength.

Cross-polarization discrimination is a measure on how well the two orthogonal polarizations are decoupled. It describes the ability of an antenna to maintain the purity of a certain polarization. Figure 12B depicts an XPD raster scan with the −0.5 and −1 dB templates defined by EUTELSAT. These templates represent the locations where the co-polarized gain level is reduced by 0.5 and 1 dB compared with its maximum.

The radiation patterns are not measured only as raster scans but also as cuts along the principle angular planes (azimuth and elevation). The EUTELSAT specifications require the full angular span of ±180° in azimuth and a smaller span (eg, ±30°) in elevation to be covered. When the radiation pattern is measured with a pre-elevation tilt different from 0°, the azimuthal span of ±180° using the motion emulator at FORTE cannot be achieved. For example, at an elevation pre-tilt of 30°, the maximum span is limited to ±160°. Figure 13 shows the transmit gain pattern of the antenna under test versus azimuth. The measurement was taken for an uplink frequency of 29.5 GHz, LHCP polarization, antenna elevation of 30°, and a radome rotation of 270°. For a better display, only the zoomed range of ±10° is depicted.

Additionally, in Figure 13, the $'29 - 25\log(\theta)'$ mask is plotted. The same mask but shifted upwards with 3 dB for the angular range between α and 9.2°, and with 6 dB for the angular range beyond 9.2° is also depicted. These relaxed masks are defined in the specifications of EUTELSAT to provide an extra margin for smaller antennas. The cross-polar pattern and the cross-polar mask (defined in the angular range α to 9.2°) are also plotted in Figure 13. The positions where the measured patterns violate the regulatory masks can be easily found by inspecting Figure 13.

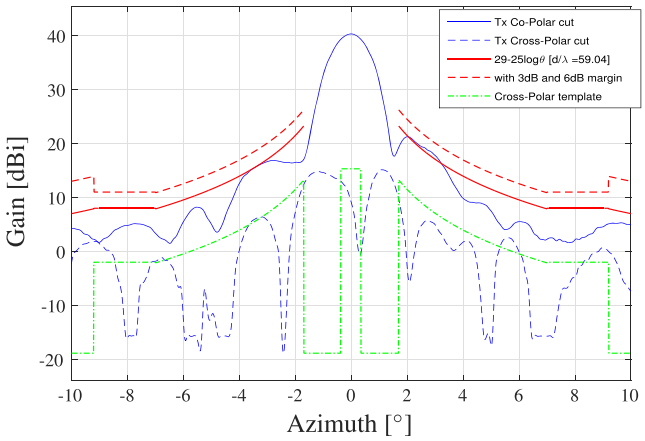

FIGURE 13 Transmit azimuth plane cut for antenna elevation 30°, frequency 29.5 GHz, left-hand circular polarization, and radome rotation 270°. A zoomed angular range of ±10° is depicted for the sake of a better display [Colour figure can be viewed at wileyonlinelibrary.com]

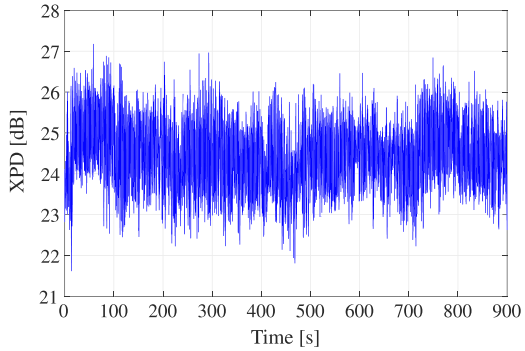

(A) Cross-polarization discrimination (XPD) of the SOTM antenna under test when tested on the maritime Class A proposed standard motion profile.

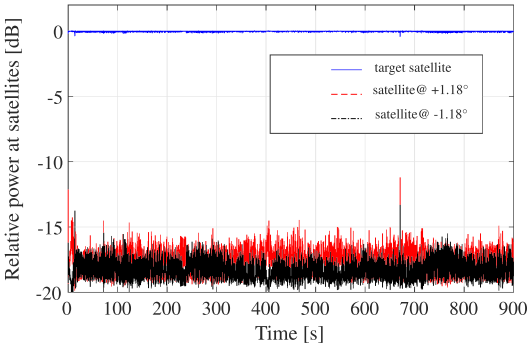

(B) Adjacent Satellite Interference (ASI) at satellite positions ±1.18° of the SOTM antenna under test when tested on the maritime Class A proposed standard motion profile. The ASI is presented as normalized power levels relative to the line of sight value at the target satellite.

FIGURE 14 Cross-polarization discrimination and Adjacent Satellite Interference. SOTM, Satcom on-the-move [Colour figure can be viewed at wileyonlinelibrary.com]

6.2.4 | Dynamic tests

In the dynamic tests, the performance of the SOTM terminal are evaluated while being on-the-move. The terminal is mounted on the motion emulator, which replays a motion profile. As described in Section 3.2, the antenna de-pointing is measured along the motion profile. Moreover, the XPD and the ASI are measured as well.

Figure 14A, shows the evolution of the XPD when the terminal is tested with the maritime Class A proposed standard motion profile. The XPD has an average of 24 dB and a standard deviation of 0.7 dB.

Adjacent Satellite Interference is measured for three satellite positions specified by EUTELSAT: 1.18°, 2.36°, and 3.53°. The power normalized to the line of sight level received at the target satellite at 0° is plotted in Figure 14B for adjacent satellite positions of ±1.18° as an example.

Figure 14B shows that, in the worst case, the adjacent satellite at +1.18° receives a power level 11 dB below the power level received when the SOTM antenna exactly points towards the target satellite. In the best case, the level is more than 19 dB lower.

Figure 15A shows the time evolution of the antenna de-pointing along azimuth and elevation for the maritime Class A proposed standard motion profile. According to EUTELSATs specifications, the antenna de-pointing must not exceed 0.4° under all circumstances. As seen from Figure 15A, the antenna de-pointing does not exceed 0.4° in any case. Therefore, the antenna is compliant with EUTELSATs specifications. Figure 16A shows the CDF of the de-pointing estimation results in Figure 15A. It can be seen that the antenna de-pointing, in azimuth and in elevation, does not exceed 0.4° in any case.

If the antenna is tested using the land mobile Class A proposed standard motion profile, the de-pointing estimation results depicted in Figure 16A are obtained. The antenna de-pointing exceeds 0.4° in azimuth and in elevation. This antenna is not equipped with the transmit mute functionality. For this reason, it transmits although the de-pointing exceeds 0.4°. From Figure 16A, it is obvious that the antenna does not fulfill the requirement of EUTELSAT for the land mobile Class A motion profile. However, by investigating the statistics of the de-pointing estimation results, the decision for the antenna to be approved or not can drastically change. Figure 16B shows the CDF of the de-pointing estimation results in Figure 16A. It can

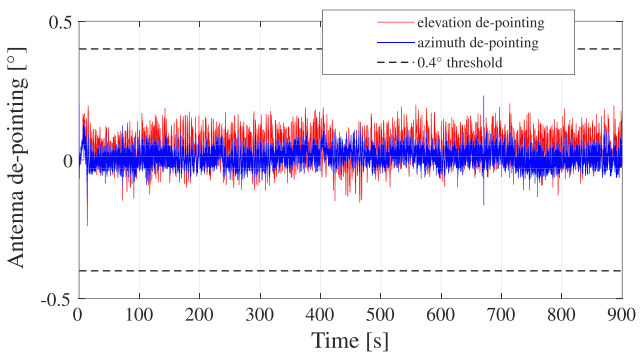

(A) De-pointing estimation results of the SOTM antenna under test when tested with the maritime Class A proposed standard motion profile. The antenna de-pointing does not exceed 0.4°, which is the limit specified by EUTELSAT, in any case.

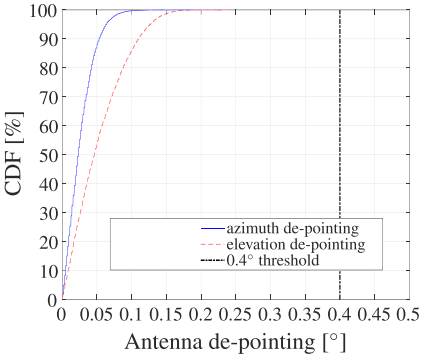

(B) The CDF of antenna de-pointing when the antenna under test is tested with the maritime Class A proposed standard motion profile. The antenna de-pointing does not exceed 0.4°, which is the limit specified by EUTELSAT, in any case.

FIGURE 15 Antenna de-pointing estimation time sequence and cumulative distribution function (CDF) for the maritime Class A proposed standard motion profile. SOTM, Satcom on-the-move [Colour figure can be viewed at wileyonlinelibrary.com]

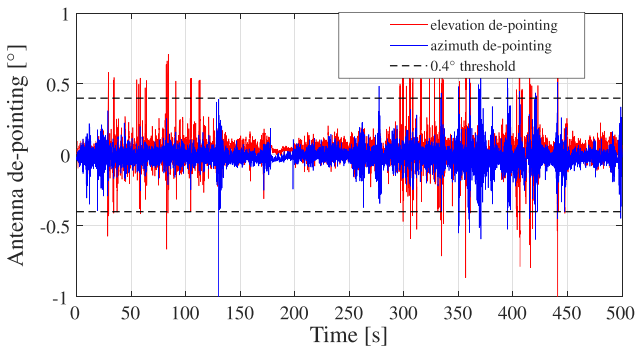

(A) De-pointing estimation results of the SOTM antenna under test when tested with the land mobile Class A proposed standard motion profile. The antenna de-pointing exceeds 0.4° which is the limit specified by EUTELSAT.

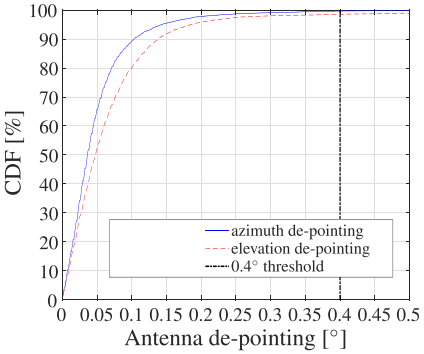

(B) The CDF of antenna de-pointing when the antenna under test is tested with the land mobile Class A proposed standard motion profile. Azimuth de-pointing exceeds the 0.4° limit only in 0.34% of the time and elevation de-pointing in 1.5%.

FIGURE 16 Antenna de-pointing estimation time sequence and cumulative distribution function (CDF) for the land mobile Class A proposed standard motion profile. SOTM, Satcom on-the-move [Colour figure can be viewed at wileyonlinelibrary.com]

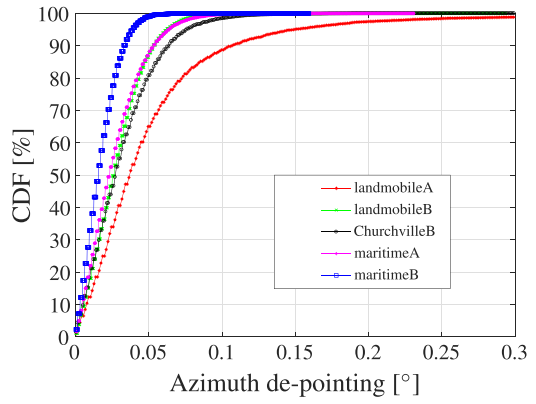

(A) CDF of azimuth de-pointing of the SOTM antenna under test when tested on different motion profiles.

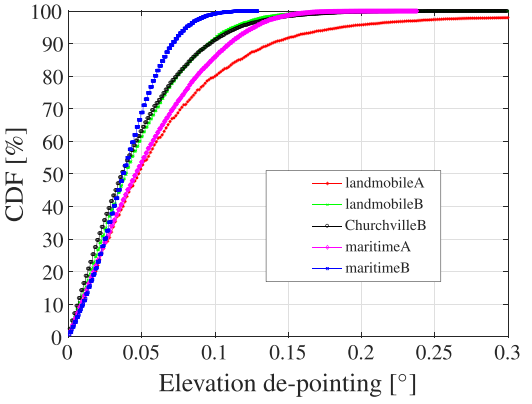

(B) CDF of elevation de-pointing of the SOTM antenna under test when tested on different motion profiles.

FIGURE 17 Cumulative distribution function (CDF) of the de-pointing estimation of the Satcom on-the-move (SOTM) antenna under test when tested on different motion profiles. The results of the well-known Churchville B motion track are also presented [Colour figure can be viewed at wileyonlinelibrary.com]

be seen that the antenna de-pointing exceeds 0.4° only in 0.34% of the time in azimuth direction and in 1.5% of the time in elevation direction. This is approximately 1.7 and 7.5 seconds in the 500 seconds long land mobile Class A motion profile. This fact might change the decision of the operator and the antenna might be approved for the land mobile environment as well.

The CDFs of antenna de-pointing are plotted for the different motion profiles in Figure 17A,B for azimuth and elevation, respectively. The proposed standard motion profiles for the land mobile and the maritime environments as well as for the Churchville B motion track are included.

It can be seen from Figure 17 that the maritime Class B motion profile is the easiest for the antenna to track and the land mobile Class A motion profile is the most challenging. This matches the findings in Section 4.

7 | CONCLUSION

In this paper, state-of-the-art SOTM standards and existing type approval procedures were reviewed and compared. This was followed by an investigation of the capabilities of the existing environments used for SOTM testing. In a laboratory environment, the SOTM terminal is tested in conditions similar to those found in the field of operation, yet without the involvement of operational satellites. As an example of a laboratory environment for SOTM testing, the framework of testing SOTM terminals at the Fraunhofer FORTE[26] was presented. As a major contribution of this paper, motion profiles were developed and are proposed to be used as a standard for SOTM testing. The proposed standard motion profiles were developed for the land mobile and the maritime environments. Standard motion profiles offer a fair basis to compare the performance of different terminals. The major satellite operators in the GVF-MRA working group showed an interest to support the deployment of the proposed profiles widely in their SOTM testing recommendations. As a result, the SOTM testing procedures of the Global VSAT Forum (GVF-105) were updated by adding the definition process of the proposed standard motion profiles. It is highly recommended that the satellite operators widely start to apply the GVF-105 test recommendations along with the GVF-SOMAP requirements and consider them in their type approvals. This will lead to an enhancement of the whole SOTM value chain through a unified type approval procedure and a unique set of regulatory limits to which all members can easily refer. Standard shadowing profiles were also proposed and developed for the land mobile environment based on an image processing approach. The definition of the proposed motion and shadowing profiles in addition to the repeatability that is guaranteed at the testing laboratories offer a comprehensive environment to test the performance of the SOTM terminal with respect to the test methodology proposed in this paper. In an example test scenario, a Ka-band SOTM terminal with a 60-cm dish antenna was tested at FORTE. The recommendations in GVF-105 and the specifications of EUTELSAT were applied in the test. An excerpt of the results was presented to demonstrate how good the antenna is in accordance with the specifications. The results help to show the points of strength and weakness of the terminal and help the designers in its development process.

ACKNOWLEDGEMENTS

The definition of standard motion profiles was conducted in the context of a project funded by the European Space Agency (ESA). Website: https://artes.esa.int/projects/mtn-ccn2 `https://artes.esa.int/projects/mtn-ccn2`.

ORCID

Mostafa Alazab Elkhouly http://orcid.org/0000-0002-7008-6458

REFERENCES

1. Alazab M, Raschke F, Landmann M, Jarrold M, Hartshorn D, Robinson C. *Standard definition for SOTM terminals.* An ESA ARTES 1 project. https://artes.esa.int/funding/standards-preparation-sotm-terminals-1a096-expro-plus; 2016.
2. Jing Z, Roy S. Improving link layer performance on satellite channels with shadowing via delayed two-copy selective repeat ARQ. *IEEE J Sel Areas Commun.* 2004;22(3):472-481.
3. Rawlins M. *Preventing harmful interference to satellite systems.* EUTELSAT Communications; 2013.
4. FCC. *Vehicle-mounted earth stations (VMES) FCC25p226).* Tech. Rep. 2010-245, Federal Communications Commission (FCC); 2010.
5. ETSI. ETSI EN 302 977 v 1.1.2, satellite earth stations and systems (SES). Harmonized EN for Vehicle-Mounted Earth Stations (VMES) operating in the 14/12 GHz frequency bands covering essential requirements under article 3.2 of the R&TTE directive; 2008.
6. Global VSAT Forum. *Performance and test guidelines for type approval of comms on the move mobile satellite communications terminals.* GVF, Tech. Rep. GVF-105; 2016.
7. Global VSAT Forum. *Satellite operators minimum antenna performance (SOMAP).* GVF, Tech. Rep.; 2017.
8. Alazab M, Rieche M, Del Galdo G, et al. On-earth performance evaluation of Satcom on-the-move (SOTM) terminals. In: Military Communications Conference; 2013:634-640; San Diego, CA.
9. Brunnenmeyer D, Mills S, Patel S, Suarez C, Kung L. Ka and Ku operational considerations for military Satcom applications. In: Military Communications Conference; 2012:1-7; Orlando, FL.
10. ETSI. *ETSI EN 302 340 v 1.1.1, satellite earth stations and systems (SES).* Harmonized EN for Satellite Earth Stations on board Vessels (ESVs) operating in the 11/12/14 GHz frequency bands allocated to the Fixed Satellite Services (FSS) covering essential requirements under article 3.2 of the R&TTE directive; 2008.

11. Beljour H, Foresta S, Hoffmann R, et al. Army Satcom OTM full elevation performance characterization. In: Military Communications Conference; 2011:1964-1967; Baltimore, MD.
12. Balanis C. *Antenna Theory: Analysis and Design*. 4th ed.: Wiley; 2016.
13. Siegert G, Felber W, Raschke F, et al. Advances of far field range for SatCom on-the-move terminals. In: Advanced Satellite Multimedia Systems Conference; 2013:428-435; Livorno, Italy.
14. Alazab M, Raschke F, Landmann M, Jarrold M, Hartshorn D, Robinson C. *Mobile tracking needs, contract change notice 2*. An ESA ARTES 5.1 project extension. https://artes.esa.int/projects/mtn-ccn2; 2016.
15. ©Fraunhofer IIS. *The mobile tracking needs (MTN) database*. https://motiondb.iis.fraunhofer.de/cmtn/main/
16. Karaliopoulos MS, Pavlidou FN. Modeling the land mobile satellite channel: a review. *Electron Commun Eng J*. 1999;11(5):235-248.
17. Prieto-Cerdeira R, Perez-Fontan F, Burzigotti P, Bolea-Alamañac A, Sanchez-Lago I. Versatile two-state land mobile satellite channel model with first application to DVB-SH analysis. *Int J Satell Commun Networking*. 2010;28:5-6.
18. Fontan FP, Vazquez-Castro M, Cabado CE, Garcia JP, Kubista E. Statistical modeling of the LMS channel. *IEEE Trans Veh Technol*. 2008;57(2):2787-2790.
19. Scalise S, Ernst H, Harles G. Measurement and modeling of the land mobile satellite channel at Ku-band. *IEEE Trans Veh Technol*. 2001;50(6):693-703.
20. Kubista E, Fontan FP, Castro MAV, Buonomo S, Arbesser-Rastburg BR, Baptista JPVP. Ka-band propagation measurements and statistics for land mobile satellite applications. *IEEE Trans Veh Technol*. 2000;49(3):973-983.
21. Hofmann C, Schwarz R, Knopp A. SOTM measurements for the characterization of the wideband mobile satellite channel at Ku-band. In: International Conference on Systems, Communications and Coding; 2015; Hamburg, Germany. 1-8.
22. Ihlow A, Arndt D, Topf F, Rothaug C, Wittenberg T, Heuberger A. Photogrammetric satellite service prediction correlation of RF measurements and image data. In: IEEE International Symposium on Broadband Multimedia Systems and Broadcasting (BMSB); 2011:1-6; Nuremberg, Germany.
23. EUTELSAT. Type approval characterization procedures. *EUTELSAT*. 2017; ESOG 120, Issue 7.0, 09.04.2018.
24. EUTELSAT. Earth station miniumum technical and operational requirements, standard M EESS 502. EUTELSAT issue 14, rev.0; 2011.
25. Bayer H, Krauss A, Stephan R, Hein M. A dual-band multimode monopulse tracking antenna for land-mobile satellite communications in Ka-band. In: The 6th European Conference on Antennas and Propagation (EuCAP); 2012:2357-2361; Prague, Czech Republic.
26. The Fraunhofer Facility for Over-the-Air Research and Testing (FORTE). https://www.iis.fraunhofer.de/en/profil/standorte/forte.html

Mostafa Alazab Elkhouly was born in 1988. He graduated with BSc from the German University in Cairo in 2010. He then finished his MSc in Communications and Signal Processing at the Technische Universität Ilmenau in 2012. From 2012 to 2017 he worked as a research fellow at the Technische Universität Ilmenau. Since June 2017, he joined the Fraunhofer Institute for Integrated Circuits IIS in Germany as a research associate. His field of interest is satellite communications with a special focus on mobile satellite applications. He is currently involved in projects with the European Space Agency where Fraunhofer IIS develops a standard testing environment for SOTM terminals. He is currently registered as a PhD student at the Technische Universität Ilmenau, Germany.

Jonas König was born in Berlin, Germany, in 1986. He received his BSc and MSc degree in electrical engineering and information technology from Technische Universität Ilmenau, Germany, in 2009 and 2011, respectively. Since 2011, he is with the Institute for Information Technology at Technische Universität Ilmenau. In 2017, he additionally joined the Fraunhofer Institute for Integrated Circuits. His current research interests include wireless propagation, antenna arrays, direction-finding, and channel modeling.

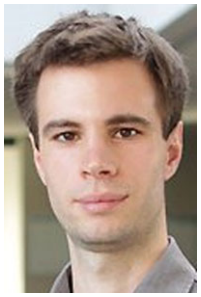

Niklas Beuster received the BSc and MSc degrees in electriengineering and information technology from Technische Universität Ilmenau, Germany, in 2014 and 2016, respectively. He is currently a research fellow with Institute for Information Technology, Technische Universität Ilmenau. His research focus is on radio frequency measurements and signal processing. He did hardware and software development for the SatCom testbed at FORTE and investigated measurement accuracy of the facility. Currently, he is working on UHF RFID Readers and Tags in a cooperative research project.

Florian Raschke received the degree Dipl.-Ing. from the Dept. of Electrical Engineering and Information Technology of the Technische Universität Ilmenau in November 2010. Since December 2010, he worked as a research assistant in the Wireless Distribution Systems department of Fraunhofer IIS. During that time, he was deeply involved with the design and integration of the SatCom testbed at FORTE. In several projects, he gained experience in developing and testing SatCom-on-the-move systems and had been in charge of an over-the-air research and testing facility. Currently, he is working as a systems engineer in the development of SatCom-on-the-move systems for Airbus Defence and Space.

Alexander Ihlow received the Dipl.-Ing. degree in electrical engineering and information technology from Technische Universität Ilmenau, Germany, in 1999, and the Dr.-Ing. degree from Otto von Guericke University Magdeburg, Germany, in 2006. Since 2008, he has been with the Institute for Information Technology, Technische Universität Ilmenau, as scientific staff member. His current research interests include signal processing, wireless communications, and measurement and testing technology.

Colin Robinson serves as the GVF-MRA chairman and is a lifetime member of the IEEE and a NARTE Certified EMC Engineer. He received his Higher National Certificate (HNC-EE) from the Ministry of Aviation College in the UK (US Equivalence BSEE). Mr. Robinson has over thirty years experience in the design, test and certification of an extensive range of antenna systems employed in aircraft, marine, terrestrial, and spacecraft communication applications with leading aerospace organizations including the Royal Aircraft Establishment (RAE Farnborough UK now DERA), Boeing Company, Emerson & Cuming (a W.R Grace Company), and General Dynamics Satcom Technologies. Most recently, Mr. Robinson's focus has been directed towards the satellite communications sector regarding VSAT antenna systems. Mr. Robinson has been involved with the type approval of close to one hundred VSAT antenna systems for satellite operators located in the USA and throughout Europe and Asia. Mr. Robinson has led the effort that resulted in the generation of a number of the GVF MRA documents including GVF-101, GVF-104, and GVF-105 documents. Mr. Robinson is an Authorized Test Entity (ATE) for the Global VSAT Forum. He is the holder of several US patents related to VSAT antenna systems.

Raul Orus-Perez received his Physics bachelor on 2000 from the University of Barcelona (UB), Spain, followed by PhD studies in Aerospace Science and Technology in the Technical University of Catalonia (UPC) inside the gAGE/UPC research group. In 2006, he was awarded with a postdoctoral research fellowship with the European Space Agency (ESA/ESTEC), Noordwijk, The Netherlands in the Electromagnetics and Space Environment Division on Ionospheric effects on GNSS systems. After one year as researcher inside gAGE-NAV UPC spin-off, in 2010, he joined ESA/ESTEC as a propagation engineer working in activities related to radiowave propagation in troposphere and ionosphere mainly for GNSS and other ESA projects.

Fritz Schurig was born in 1954. He is in charge of Approval, Operations and Testing of Earth Stations at EUTELSAT, France since Sept 1986. He graduated at the engineering College of DBP at Dieburg, Germany in 1978. In 1978, he started working as a telecom engineer at the Telecommunications Office in Kaiserslautern, Germany. In 1981-82, he worked in the field of telecom training for ITU (International Telecommunication Union) in Jordan and Fiji. In 1983, he returned to the FTZ (Central Engineering Office of DBP) in Darmstadt, Germany. Since 1986, he has been working at EUTELSAT, France.

Andreas Knopp received the B. Eng (1999), the MSc (2002), and PhD (2008) degrees (with distinction) in radio communications from the Bundeswehr University Munich. He is now the chair holder of signal processing and a Full Professor with the Department of Electrical Engineering and Information Technology. Prior to taking up the faculty position in 2014, Andreas has gained expertise as a practitioner in satellite communications while holding several positions as a satellite engineer, project manager, and program manager. Among others, he served in the German central development and procurement agency for Military Communications Equipment and Technology. His current research interests include satellite network integration, digital signal processing for HTS, signal parameter estimation, and radio waveform design. Andreas is an IEEE Senior Member, a member of AFCEA, and a member of the German engineers association VDE.

Albert Heuberger received his Dipl.-Ing. degree in electrical engineering from Erlangen University before joining Fraunhofer IIS as research associate in the area Radio Frequency in 1987. He became head of the Communications department and was in charge of research on Localization and Communication. Receiving his doctorate in Erlangen in 2005, he was appointed university professor in 2008 at the Technische Universität Ilmenau for the research area Wireless Distribution Systems / Digital Broadcasting. On October 1, 2011, Albert Heuberger was named Executive Director of Fraunhofer IIS, which ranks first among the Fraunhofer Institutes concerning headcount and revenues. As the main inventor of mp3 and universally credited with the codevelopment of AAC audio coding standard, Fraunhofer IIS has reached worldwide recognition. It provides research services on contract basis and technology licensing.

Markus Landmann was born in Zeitz, Germany, in 1977. He is technical supervisor and head of the Over the Air Testing Group in the Wireless Distribution Systems Dept.—received the Dipl.-Ing. degree and Dr.-Ing. degree in electrical engineering (information technology) from the Technische Universität Ilmenau, Germany, in 2001 and 2008, respectively. From 2001 to 2003, he worked as a research assistant and instructor at Technische Universität Ilmenau. In 2004, he was developing advanced antenna array calibration methods and high resolution parameter estimation algorithm (RIMAX) for propagation studies at MEDAV Company. In 2005, he was visiting researcher and instructor at Tokyo Institute of Technology (Takada Laboratory) in the field of channel measurement and estimation techniques. From 2006 to 2008, he was finalizing his PhD thesis while a research assistant and instructor at Technische Universität Ilmenau. Between 2008 and 2009, his projects were in wireless propagation, channel modeling, and array signal processing for Technische Universität Ilmenau and Tokyo Institute of Technology. In 2010, he started working for Fraunhofer IIS within the Department Wireless Distribution System / Digital Broadcasting headed by Professor Giovanni Del Galdo. He is mainly responsible for the Facility for Over the Air Research and Testing.

Giovanni Del Galdo studied telecommunications engineering at Politecnico di Milano. In 2007, he received his doctoral degree from Technische Universität Ilmenau on the topic of MIMO channel modeling for mobile communications. He then joined Fraunhofer Institute for Integrated Circuits IIS working on audio watermarking and parametric representations of spatial sound. Since 2012, he leads a joint research group composed of a department at Fraunhofer IIS and, as a full professor, a chair at TU Ilmenau on the research area of wireless distribution systems and digital broadcasting. His current research interests include the analysis, modeling, and manipulation of multidimensional signals, over-the-air testing for terrestrial and satellite communication systems, and sparsity promoting reconstruction methods.

How to cite this article: Alazab Elkhouly M, König J, Beuster N, et al. Standardized testing conditions for satellite communications on-the-move (SOTM) terminals. *Int J Satell Commun Network*. 2019;37:163–182. https://doi.org/10.1002/sat.1272